XVI International Conference on Durability of Building Materials and Components
DBMC 2023, China
K.F. Li and D.P. Fang (Eds)

Evaluation of Alteration in Cement Paste Due to Calcium Leaching with Integrated CT-XRD Method and Its Effect on Ionic Diffusions

Yingyao Tan[1], Takafumi Sugiyama[2] and Katsufumi Hashimoto[1]

[1] Environmental Material Engineering Laboratory, Graduate School of Engineering, Hokkaido University, Sapporo Japan, yingyao.tan.x0@elms.hokudai.ac.jp (Yingyao Tan. corresponding author)

[2] Environmental Material Engineering Laboratory, Faculty of Engineering, Hokkaido University, Sapporo Japan, takaf@eng.hokudai.ac.jp (Takafumi Sugiyama), hashimoto.k@eng.hokudai.ac.jp (Katsufumi Hashimoto)

Abstract. *In 2011, Tohoku earthquake and subsequent tsunami hit Fukushima Daiichi Nuclear Power Plant, and they lead to Fukushima nuclear disaster. For more than a decade after the disaster, concrete materials in submerged structures of nuclear power plants have been chronically in contact with water and resulted in calcium leaching. To assess the alteration of the concrete property, it's necessary to evaluate the permeability change due to calcium leaching and its effect on radioactive ion diffusion. In this study, small scale cylindrical cement paste specimens with 3mm in diameter and 6mm in height were prepared with water to cement ratios of 0.5 and 0.6 respectively, and they were tested in the static leaching. Specimens were subjected to carbonation before immersed into deionized water for different periods. CT image of each specimen at a resolution of 2.46μm/voxel was acquired in SPring-8, Hyogo, Japan. Combining CT images and X-ray diffraction data, dissolution front of portlandite under different leaching periods was determined, and the time dependent development law of dissolution front was evaluated. Introducing Buil's model as a local equilibrium, time and position dependent porosity of cement paste due to leaching was calculated and correspondingly diffusion coefficient of Sr ion in the numerical simulation was modified. Simulative results on Sr ion diffusivity for 10-year showed the impact of carbonation followed by leaching on radioactive ion diffusion.*

Keywords: *Synchrotron X-ray CT, X-ray Diffraction, Leaching Deterioration, Sr Diffusion, Simulation.*

1 Introduction

Concrete is widely used for nuclear power plants and facilities in underground environments due to its stable chemical properties fulfill the requirement of structural stability. However, in long-term repository of low-level radioactive wastes, water saturated condition causes potential degradation of the concrete barriers (Haga et al 2005). Tohoku earthquake led to Fukushima nuclear disaster in 2011. In the past decade, underground concrete structure has been in contact with water and resulting in calcium leaching, while diffusion of radioactive ion from wastewater in concrete structure also occurs simultaneously. Before the accident the concrete used in the nuclear plants had been exposed to air for longer periods of time. Generally, property of concrete is altered with carbonation, which collectively changes the pore structure of concrete and further affects diffusion of radioactive ion through it (Müllauer et al 2012). For assessing the current condition of nuclear power plant and providing reference for future maintenance, it's necessary to evaluate the permeability change due to calcium leaching as well as carbonation and its effect on radioactive ion diffusion. As a non-destructive and non-invasive

imaging technique, X-ray microcomputed tomography (CT) was applied in this study to detect the 3D geometry of the specimens (Darma et al 2013). Pore structure of specimen changes with release of calcium ion from hydration products. To identify the mechanism, random walk algorithm was introduced to obtain tortuosity of pore structure. Considering the combined effects of calcium releasing followed by the pore structure change, numerical calculation based on the Fick's Law was carried out to simulate 10-year radioactive ion diffusion in concrete.

2 Experiments

2.1 Carbonation and Non-accelerated Leaching Tests

Tiny cylindrical cement pastes specimens with 3mm in diameter and 6mm in height were prepared for the natural leaching test. Ordinary Portland cement (OPC) was used and specimen series with water to cement (w/c) ratio equal to 0.5 and 0.6 were prepared separately. By mass, the oxide composition of OPC was 65.01% CaO, 21.41% SiO_2, 4.84% Al_2O_3, 3.20% Fe_2O_3, 1.08% MgO, and 2.02% SO_3. Cement paste was mixed and placed into plastic mold. Specimens was demolded after 24h and then cured by being wrapped in wet towel at 20±2℃ for four weeks. Following curing, specimens were divided into non-carbonated and carbonated series, and the specimens of carbonated series were further placed into a desiccator for 2 weeks for carbonation. In carbonation, desiccator with specimens inside was vacuumed and then carbon dioxide gas was injected subsequently. For non-accelerated leaching test, both non-carbonated and carbonated specimens were submerged in $10cm^3$ purified water filled in a plastic bottle as solvent. Leaching period of each specimen was set differently as 7 days, 15 days, 60 days and 120 days. Solvent was replaced irregularly according to the amount of released calcium ions and the concentration of calcium ions in the solvent was measured by applying inductively coupled plasma atomic emission spectroscopy (ICP). Specimens were labeled according to 'w/c ratio' + 'with or without carbonation (C or N)' + 'leaching period'. For example, specimen with w/c equals to 0.5, with carbonation and 60 days leaching period was labeled as '5C60'.

2.2 CT Imaging and In-situ XRD Measurement

Micro tomographic images were acquired at a resolution of 2.46μm/voxel using an X-ray CT system at BL28B2 in SPring-8, Hyogo, Japan (Takahashi et al 2019). During imaging, the specimen was positioned in the direction of monochromatic X-ray and exposed, followed by the capture of an X-ray camera. The experimental process is shown in the Figure 1.

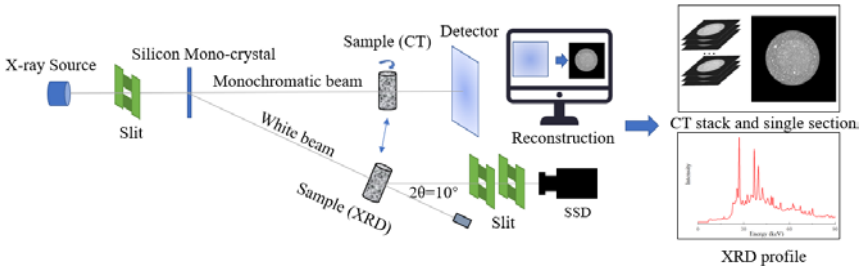

Figure 1. Schematic diagram of CT measurement and XRD measurement

To obtain porosity and 3D pore structure from CT measurement, the volume of interest (VOI)

was selected from the stack of CT images and the image binarization was applied subsequently. In the binarization process, pore structure was extracted by thresholding voxels based on their gray-level histogram as shown in Figure 2. In this study, global thresholding was used to separate the pore from the 'solid' by defining the range of grayscale (GSV) associated with the pore voxel. Porosity can be obtained by calculating the proportion of pore pixels, while pore structure can be obtained by turning GSV of pore pixels to 255 and GSV of solid pixels to 0.

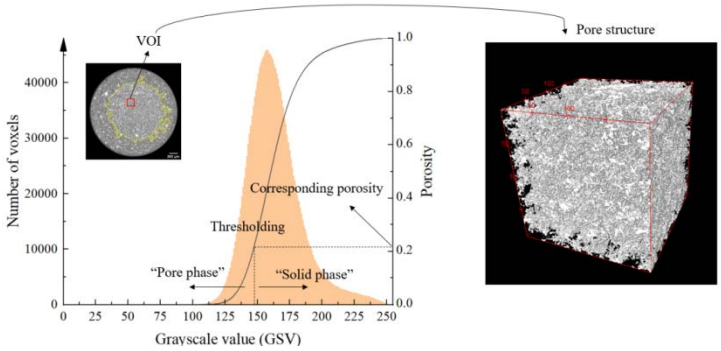

Figure 2. Schematic diagram of thresholding and 3D geometry of pore structure

In XRD measurement, the same X-ray source was used but with the use of a white X-ray. The slit system extracted only the signal from the Region of Interest (ROI), and the diffracted X-ray was captured by the solid-state detector. By comparing the acquired XRD data with the existing XRD pattern of single mineral, mineral composition of the ROI can be qualitatively analyzed.

3 Analysis

3.1 Dissolution Front of Portlandite

Figure 3 shows CT image of 6N15 and 6C120, with the following markings: right blue line shows the front of region with different GSVs while points with number label are in-situ XRD detected position and the corresponding XRD data are shown on the right. Reference pattern of portlandite and calcite are also attached for comparison.

In CT image of 6N15, points 1, 2 and 3 lie outside the front while points 4 and 5 lie inside. Peaks of portlandite signal are clearly detected inside the front while not outside, which indicates the front on the CT image is dissolution front of portlandite and dissolution of portlandite results in GSV decrease. Region inside the front is non-altered region. In CT image of 6C120, no such clear front detected and XRD signals from all points are matched well with calcite. This is due to the majority of portlandite is converted into calcite during carbonization process and the low solubility of calcite is insufficient to form a detectable dissolution front within 120 days. In addition, data from 6C0 shows that there are still a few peaks of XRD signals match with the portlandite pattern while is hardly seen in 6C120. This indicates remaining portlandite after carbonation process completely dissolved for 120s leaching process.

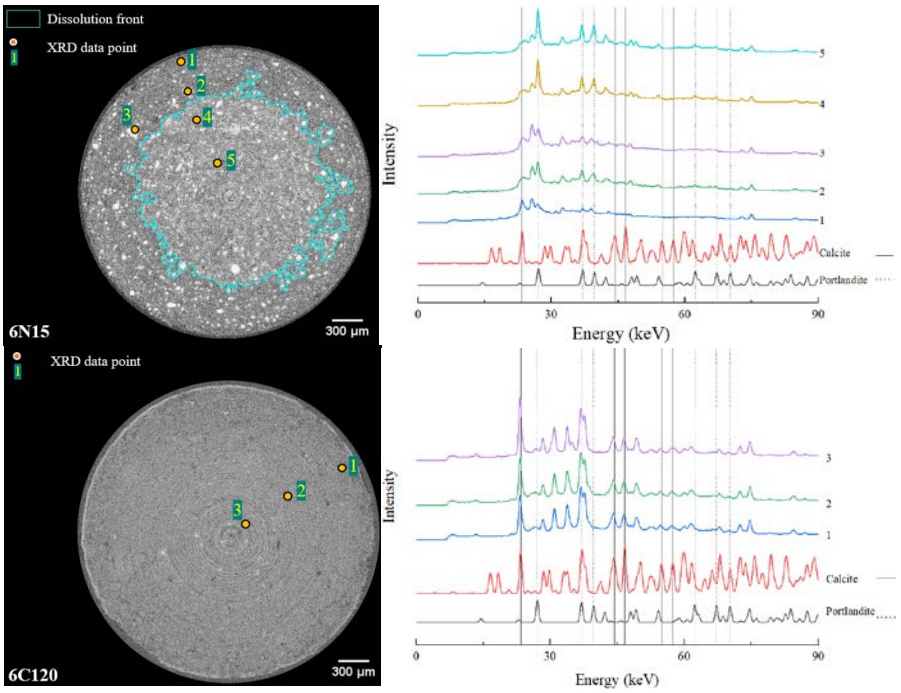

Figure 3. CT image and corresponding XRD data of 6C15 and 6C120

Dissolution front of non-carbonated specimens with different leaching period can be obtained, which are shown in Figure 4. Area of non-altered region can be obtained by counting pixels number inside the front and then multiplying it by the area of each pixel. Then, equivalent depth can be calculated by eq (1):

$$d_e = r - \sqrt{\frac{NR_e{}^2}{\pi}} \tag{1}$$

In which, r is diameter of specimen, N is number of pixels inside the front and R_e is resolution, that is 2.46μm/pixel. Equivalent depths of dissolution front are shown in Figure 5. There is basically a linear correlation between the equivalent depth and square to t.

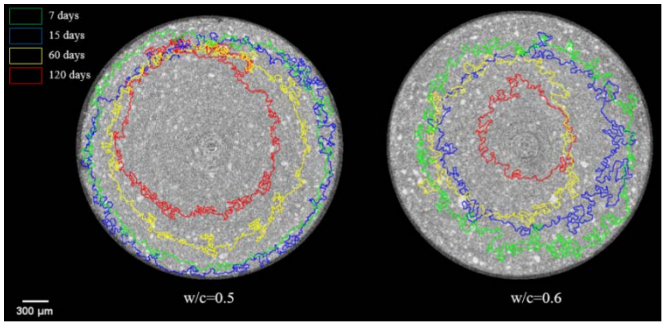

Figure 4. Dissolution front of non-carbonated specimens with different leaching period

Released calcium amount of each specimen series was measured by ICP method and is

shown in Figure 6. For non-carbonated specimen, under the assumption that all released calcium amount comes from portlandite in altered region, released calcium amount was theoretically calculated with an aid of from CT image and plotted in Figure 6. Calculated result matches well with experimental results, which means that the released calcium comes from portlandite. Little calcium released for carbonated specimen comparing with non-carbonated specimen, resulting from low solubility of calcite.

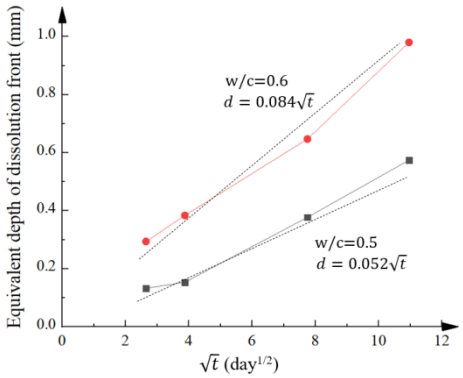

Figure 5. Dissolution fronts of non-carbonated specimens with different leaching periods

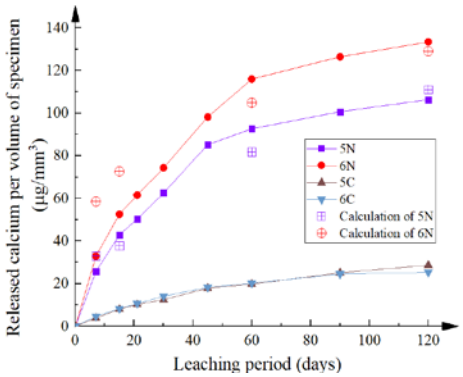

Figure 6. Accumulated released calcium per volume with different leaching periods

3.2 Calcium Release From Hydrated Cement Product

Calcium release occurs to maintain the chemical equilibrium of calcium ion between solid phase and the pore solution. Once concentration of calcium ion in pore solution decreases due to diffusion, calcium is subsequently released from portlandite and C-S-H. Buil proposed a model to describe this process in non-carbonated cement paste (Buil et al 1992). Portlandite dissolution starts first, following depletion of portlandite and inward development of dissolution front, the decalcification of C-S-H gel occurs. The speed of decalcification in C-S-H gel is related to its Ca/Si ratio which changes with calcium releasing (Carde et al 1999). Initial portlandite content in hydrated cement system and initial Ca/Si ratio in C-S-H gel can be calculated from composition of cement. While for carbonated specimens, under the assumption that all portlandite turns into calcite, calcium releases from C-S-H gel from the beginning of the leaching. Calcite and/or other types of calcium carbonate remains within specimen after decalcification or decomposition of C-S-H due to its relative low solubility.

Porosity of certain VOIs can be obtained from CT image by binarization process. Significant difference was obtained in the porosity of VOI inside and outside the dissolution front, which was due to the dissolution of portlandite (Haga et al 2005, Carde et al 1999). Lower porosity was found in carbonated specimen, resulting from the conversion of portlandite to calcite with a larger molar volume during carbonation process. In carbonated specimen, no significant differences in porosity were obtained even after 120 days leaching period, which indicates leaching effect to carbonated specimen is limited.

3.3 Effective Diffusion Coefficient with Random Walk Simulation

The diffusion process in porous media is slower than that in free liquid medium which results from the fact that Brownian motion path of a particle will be affected by obstacles in porous media (Matyka et al 2008). Relationship between diffusion coefficient in porous media and in free liquid medium (D_e and D_f) can be shown in eq (2):

$$D_e = \frac{D_f \rho_e}{\tau_D} \tag{2}$$

In which, ρ_e is effective porosity and τ_D is diffusion tortuosity. The time-dependent diffusion coefficient associated with the random Brownian motion of particles can be utilized to probe the geometry of the porous media. Quantifying diffusion tortuosity can be achieved by performing Random walk simulation in the largest percolating pore cluster (Nakashima et al 2007, Tan et al 2023). Diffusion tortuosity (τ_D) can be calculated by eq (3):

$$\langle r(t)^2 \rangle = \frac{1}{n}\sum_{i=1}^{n}\left[\left(x_i(t) - x_i(0)\right)^2 + \left(y_i(t) - y_i(0)\right)^2 + \left(z_i(t) - z_i(0)\right)^2\right]$$
$$\tau_D = \frac{D_0}{D_\infty} = \frac{\langle r(\tau)^2 \rangle_{free}}{\langle r(\tau)^2 \rangle_{pore}} \tag{3}$$

In which, $\langle r(t)^2 \rangle$ is the mean-square displacement (MSD) of walkers as a function of lattice time. n is the number of random walkers and $x_i(t)$, $y_i(t)$, and $z_i(t)$ are the 3-D coordinates of the walker's position at the time t for the ith walker. Diffusion tortuosity (τ_D) is defined as the ratio of the self-diffusion coefficient D_0 of non-absorbing walkers in free space to the long-time self-diffusion coefficient $D_\infty$of these walkers in pore space, which also can be calculated as the ratio of MSD in free space to MSD in pore space.

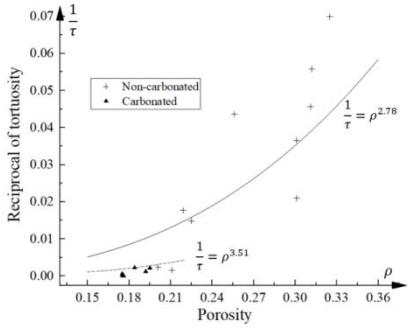

Figure 7. 1⁄τ-ρ relationship from Random walk simulation

Figure 7 shows random walk simulation result of the porosity and the reciprocal of tortuosity for extracted VOIs from both non-carbonated and carbonated specimens. Fitting curves for both plots are also given by referring from literature (Matyka et al 2008).

4 Simulations and Result

Numerical calculation simulates strontium ion (Sr ion) diffusion process for 10-year in concrete under carbonation and following leaching deterioration. Water attack results in alteration of hardened cement paste and Sr ion diffusion occurs simultaneously. Schematic diagram of calculation is shown in Figure 8. One dimension model for Sr ion diffusion in concrete was developed governed by Fick's law. In each time interval, amount of diffusing Sr ions between cells is calculated and concentration of Sr ion in each cell is updated. Amount of released calcium is estimated as shown in section 3.1 and porosity change of each cell is calculated. Sequential diffusion coefficient change of Sr ion is calculated for each cell in accordance with pore structure change which is governed by the relationship between porosity and tortuosity obtained from section 3.3. In the following time interval, diffusion of Sr ion is calculated based on the updated parameters until time reach 10-year. Diffusion coefficient of Sr ion in free liquid is 7.12×10^{-10}m^2/s, and the distribution coefficient is $K_d = 0.2$. (Johnston et al 1992)

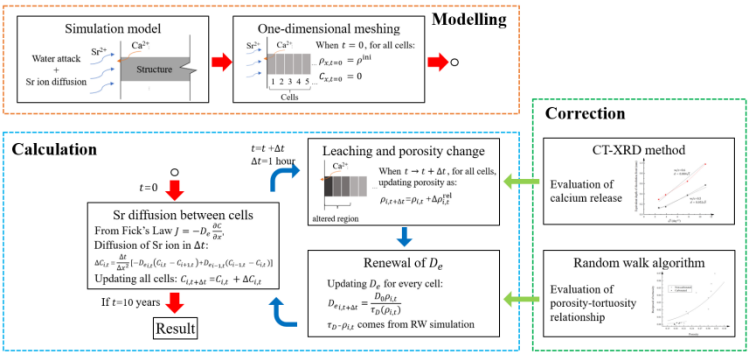

Figure 8. Schematic diagram of calculation

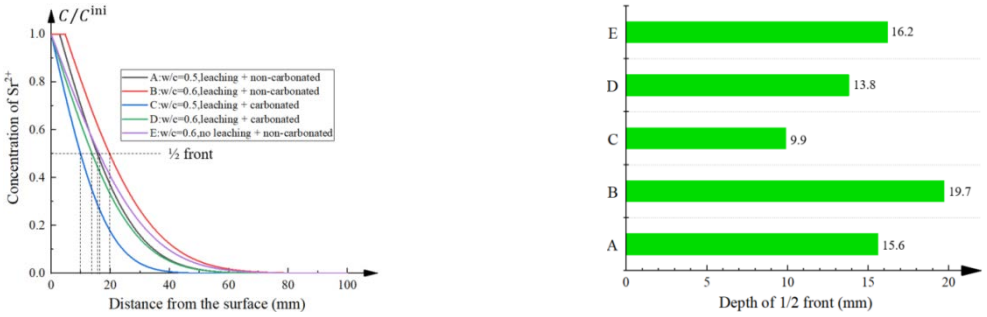

Figure 9. Concentration of Sr^{2+} in specimen after 10-year diffusion process

Result of the simulation of Sr ions diffusion after 10-year under different condition (A to E) is given in Figure 9. For comparison of varied conditions of concrete, the depth of the half concentration of Sr ions is used as the basis for evaluating the diffusion processes in different condition. Lower diffusion speed was verified in lower w/c ratio and the depth of 1/2 concentration in concrete with w/c=0.6 (B) is about 26% higher than with w/c=0.5 (A). Carbonation process also slows down diffusion of Sr ion. Comparing with non-carbonated concrete (A or B), about 30% lower depth was shown for carbonated concrete (C or D). From

the comparison of series B and D, if effect of leaching deterioration was not considered, about 19% lower depth was underestimated.

5 Conclusions

The following conclusions are drawn based on the results of this research:

- Combining the CT-XRD method and the monitoring of released calcium amount, it was found that the calcium released during leaching process mainly comes from portlandite, and the porosity change during leaching was estimated.
- Change of diffusion coefficient due to the alteration of pore structure was quantified with the porosity-tortuosity relationship by applying random walk simulation.
- Based on the Fick's Law, Sr ion diffusion model in concrete was developed. Result showed that the Sr diffusion in carbonated concrete was suppressed as compared with non-carbonated one and the leaching of calcium ions led to the increased diffusion of Sr ions after 10-year diffusion.

Acknowledgements

Part of this research was funded by the Japan Society for Promotion of the Science (JSPS KAKENHI Grant Number 21H01402) and the Nuclear Safety Research Association. The synchrotron radiation experiments were performed at the BL28B2 in SPring-8 with the approval of Japan Synchrotron Radiation Research Institute (Proposal No. 2021B1025, 2022A1662).

References

Buil, M., Revertegat, E., & Oliver, J. (1992). *A model of the attack of pure water or undersaturated lime solutions on cement*. ASTM Special Technical Publication, 1123, 227-241.

Carde, C., & Francois, R. (1999). *Modelling the loss of strength and porosity increase due to the leaching of cement pastes*. Cement and Concrete Composites, 21(3), 181-188.

Darma, I. S., Sugiyama, T., & Promentilla, M. A. B. (2013). *Application of X-ray CT to study diffusivity in cracked concrete through the observation of tracer transport*. Journal of advanced concrete technology, 11(10), 266-281.

Haga, K., Sutou, S., Hironaga, M., Tanaka, S., & Nagasaki, S. (2005). *Effects of porosity on leaching of Ca from hardened ordinary Portland cement paste*. Cement and concrete research, 35(9), 1764-1775.

Johnston, H. M., & Wilmot, D. J. (1992). *Sorption and diffusion studies in cementitious grouts*. Waste Management, 12(2-3), 289-297.

Matyka, M., Khalili, A., & Koza, Z. (2008). *Tortuosity-porosity relation in porous media flow*. Physical Review E, 78(2), 026306.

Müllauer, W., Beddoe, R. E., & Heinz, D. (2012). *Effect of carbonation, chloride and external sulphates on the leaching behaviour of major and trace elements from concrete*. Cement and Concrete Composites, 34(5), 618-626.

Nakashima, Y., & Kamiya, S. (2007). *Mathematica programs for the analysis of three-dimensional pore connectivity and anisotropic tortuosity of porous rocks using X-ray computed tomography image data*. Journal of Nuclear Science and Technology, 44(9), 1233-1247.

Tan, Y., Sugiyama, T., & Hashimoto, K. (2023). *Evaluation of transport properties of deteriorated concrete due to calcium leaching with coupled CT image analysis and random walk simulation*. Construction and Building Materials, 369, 130526.

Takahashi, H., & Sugiyama, T. (2019). *Application of non-destructive integrated CT-XRD method to investigate alteration of cementitious materials subjected to high temperature and pure water.* Construction and building materials, 203, 579-588.